

sults were essentially identical, with the only difference being in the higher resolution and greater peak separation obtained with the Multitaper method.

13. J. Park, K. A. Maasch, *J. Geophys. Res.* **98**, 447 (1993).
14. R. M. Leckie, P. N. Webb, *Geology* **11**, 578 (1983).
15. W. Ehrmann, *Palaeogeogr. Palaeoclimatol. Palaeoecol.* **139**, 213 (1998).
16. L. Sagnotti, F. Florindo, K. L. Verosub, G. S. Wilson, A. P. Roberts, *Geophys. J. Int.* **134**, 653 (1998).
17. The $\delta^{18}\text{O}$ values of *Cibicides* and most other benthic foraminifera taxa reflect on changes in both water temperature and ice-volume. For example, benthic $\delta^{18}\text{O}$ will increase by 0.25‰ for each 1°C decline in temperature. On the other hand, a doubling of Antarctic ice-sheet mass would increase ocean (and benthic) $\delta^{18}\text{O}$ by roughly 1.0‰.
18. S. C. Clemens, R. Tiedemann, *Nature* **385**, 801 (1997).
19. Although Pleistocene climate has a strong (dominant) 100-ky signal, the direct effects of eccentricity on global climate, particularly in polar regions, are considered too small to account for these changes. This and the lack of a similarly strong climate signal associated with the 400-ky eccentricity band, which has an equivalent effect on the radiation balance, are often viewed as major deficiencies of Milankovitch theory.
20. Marine organic carbon has a mean $\delta^{13}\text{C}$ of -20‰ , whereas mantle-derived CO_2 has a mean $\delta^{13}\text{C}$ of -7‰ . As a result, a sustained change in the flux of either has the potential to alter the mean $\delta^{13}\text{C}$ of the ocean, as well as pCO_2 , on 10^4 to 10^6 year time scales.
21. T. D. Herbert, *Proc. Natl. Acad. Sci. U.S.A.* **94**, 8362 (1997).
22. B. P. Flower, J. P. Kennett, *Palaeogeogr. Palaeoclimatol. Palaeoecol.* **108**, 537 (1994).
23. J. C. Zachos, B. P. Flower, H. Paul, *Nature* **388**, 567 (1997).
24. J. C. Zachos, T. M. Quinn, K. A. Salamy, *Paleoceanography* **11**, 251 (1996).
25. U. Mikolajewicz, E. Maierreimer, T. J. Crowley, K. Y. Kim, *Paleoceanography* **8**, 409 (1993).
26. G. T. Nong, R. G. Najjar, D. Seidov, W. H. Peterson, *Geophys. Res. Lett.* **27**, 2689 (2000).
27. D. A. Short, J. G. Mengel, T. J. Crowley, W. T. Hyde, G. R. North, *Quat. Res.* **35**, 157 (1991).
28. S. Rutherford, S. D'Hondt, *Nature* **408**, 72 (2000).

29. M. Pagani, M. A. Arthur, K. H. Freeman, *Paleoceanography* **14**, 273 (1999).
30. P. N. Pearson, M. R. Palmer, *Nature* **406**, 695 (2000).
31. M. E. Raymo, *Annu. Rev. Earth Planet. Sci.* **22**, 353 (1994).
32. E. N. Edinger, M. J. Risk, *Palaios* **9**, 576 (1994).
33. L. J. Lourens, F. J. Hilgen, *Quat. Int.* **40**, 43 (1997).
34. J. C. Zachos, K. C. Lohmann, J. C. G. Walker, S. W. Wise, *J. Geol.* **101**, 191 (1993).
35. M. A. Maslin, X. S. Li, M. F. Loutre, A. Berger, *Q. Sci. Rev.* **17**, 411 (1998).
36. M. E. Mann, J. M. Lees, *Clim. Change* **33**, 409 (1996).
37. We are indebted to M. Harvey for assistance in generating the Site 926 stable isotope record, and S. Crowhurst for assisting with the time series analyses and providing comments on this manuscript. We also thank B. Beitleir, J. Chapmann, and G. Koehler for technical assistance and F. Hilgen and T. Crowley for feedback on the orbital alignment anomaly hypothesis. Supported by the National Science Foundation (EAR-9725789).

14 December 2000; accepted 7 March 2001

Molecular Mechanisms of the Biological Clock in Cultured Fibroblasts

Kazuhiro Yagita,¹ Filippo Tamanini,² Gijsbertus T. J. van der Horst,² Hitoshi Okamura^{1*}

In mammals, the central circadian pacemaker resides in the hypothalamic suprachiasmatic nucleus (SCN), but circadian oscillators also exist in peripheral tissues. Here, using wild-type and *cryptochrome* (*mCry*)-deficient cell lines derived from *mCry* mutant mice, we show that the peripheral oscillator in cultured fibroblasts is identical to the oscillator in the SCN in (i) temporal expression profiles of all known clock genes, (ii) the phase of the various mRNA rhythms (i.e., antiphase oscillation of *Bmal1* and *mPer* genes), (iii) the delay between maximum mRNA levels and appearance of nuclear mPER1 and mPER2 protein, (iv) the inability to produce oscillations in the absence of functional *mCry* genes, and (v) the control of period length by mCRY proteins.

In the mouse, the core oscillator of the master circadian clock in the SCN is composed of interacting positive and negative transcription-translation feedback loops (1–3), which involve three homologs of the *Drosophila* gene *period* (*mPer1*, *mPer2*, and *mPer3*), two cryptochrome genes (*mCry1* and *mCry2*), and the transcriptional activator genes *Clock* and *Bmal1* (1, 2, 4). A key step in this feedback loop is the shutdown of CLOCK- and BMAL1-driven transcription by mCRY proteins (4). To keep pace with the solar day-night cycle, the master clock can be entrained by light received through photoreceptors in the retina (5). Molecular oscillators also exist

in peripheral tissues, where they cycle with a 6- to 8-hour delay with respect to the central pacemaker (6–8). In contrast to *Drosophila* and zebrafish, mammalian peripheral clocks do not directly respond to light but are synchronized by the SCN by neuronal and/or humoral signals (9). In vitro, brief treatment of cultured cells with various compounds [serum, forskolin, 12-*O*-tetradecanoylphorbol 13-acetate (TPA), adenosine 3',5'-monophosphate (cAMP), or dexamethasone] induces rhythmic expression of the clock genes *Per1*, *Per2*, and *Cry1* and the circadian transcription factor gene *dbp* for two to three cycles (6, 10–12).

To investigate whether the molecular makeup of the peripheral oscillator in cultured fibroblasts resembles that of the core oscillator in the SCN, we determined the expression profiles of all known clock genes in cultured rat-1 fibroblasts over a period of 3 days (13). To trigger the oscillations, we used the vasoconstricting peptide endothelin-1

(ET-1) (14), which activates the protein kinase C–mitogen-activated protein kinase cascade and cAMP response element-binding protein (CREB) phosphorylation (15). This treatment induces a rapid, robust increase in *Per1* and *Per2* gene expression, followed by a sharp reduction in corresponding mRNA levels and subsequent synchronous cycling of *Per1*, *Per2*, *Per3*, and *dbp* mRNAs (Fig. 1) (16, 17). Also, robust cycling of *Bmal1* mRNA was observed, with mRNA levels accumulating antiphase to *Per* and *dbp* mRNA cycles. *Clock* mRNA levels were constant at all time points examined. In addition, *Cry1* expression showed rhythmicity, peaking 4 to 8 hours after *Per* mRNAs (16). These data demonstrate that ET-1 can induce circadian gene expression in cultured rat-1 cells and that the temporal expression patterns of *Per*, *Bmal1*, *Cry1*, and *dbp* genes (all rhythmically expressed) as well as the *Clock* gene (constitutively expressed) match those in the SCN (1, 18). Casein kinase Iε (*CKIε*) and *Cry2* genes did not show apparent rhythmic expression in rat-1 cells, a finding consistent with the observation that in the SCN *CKIε* is constitutively expressed (19) and cycling of mouse *Cry2* is weak (18) or not detectable (20).

Next, we analyzed by immunocytochemistry the PER1 and PER2 protein expression profiles in these cells. Nuclear staining occurred 26 to 28 hours after treatment, indicating that mPER1 and mPER2 protein cycles follow the rhythm of *Per1* and *Per2* mRNA expression with a 4- to 8-hour delay (Fig. 2), as in the SCN (21). In addition, pronounced PER1 and PER2 nuclear staining was found 1.5 hours after ET-1 treatment (Fig. 2) (22), suggesting that ET-1 causes rapid synthesis of PER1 and PER2 and translocation of these proteins into the nucleus. This nuclear PER2 may up-regulate *Bmal1* expression and down-regulate *Per* gene expression 4 hours after ET-1 treatment (Fig. 1)

¹Division of Molecular Brain Science, Department of Brain Sciences, Kobe University Graduate School of Medicine, Chuo-ku, Kobe 650-0017, Japan. ²Center for Biomedical Genetics, Department of Cell Biology and Genetics, Erasmus University, Post Office Box 1738, 3000 DR, Rotterdam, Netherlands.

*To whom correspondence should be addressed. E-mail: okamurah@kobe-u.ac.jp

REPORTS

(16). The latter effect may also involve the CRY proteins.

We next used spontaneously immortalized (mutant) mouse embryonic fibroblasts (MEFs) from wild-type and *mCry1^{-/-}mCry2^{-/-}* mice to test the role of *mCry* genes in the fibroblast clock (23, 24). Treatment of wild-type MEFs with ET-1 resulted in a temporary induction of *mPer1* gene expression within 1 hour, followed by synchronous cycling of *mPer1* and *dbp* mRNA (Fig. 3A) (17). Four hours after stimulation, increased *Bmal1* mRNA levels were observed (Fig. 3A), which most likely requires synthesis and nuclear translocation of the mPER2 protein and subsequent rhythmic expression of *Bmal1* mRNA antiphase to *mPer1* and *dbp*. Thus, as in rat-1 cells, ET-1 can induce circadian gene expression in MEFs. In marked contrast, ET-1 treatment of *mCry1^{-/-}mCry2^{-/-}* MEFs did not result in rhythmic expression of *mPer1*, *Bmal1*, or *dbp* genes (Fig. 3, B and C). Instead, as in the SCN, *mCry1^{-/-}mCry2^{-/-}* MEFs showed continuously accumulating *mPer1* mRNA and low levels of *Bmal1* mRNA, respectively. The absence of mCRY proteins also resulted in constant high expression of the *dbp* gene. Because *mCry1^{-/-}mCry2^{-/-}* MEFs express *ET-A receptor* mRNA (25), the lack of rhythmic gene expression in these cells is unlikely to result from improper activation of signal transduction pathways, but rather is caused by the absence of mCRY proteins. Interestingly, *mCry1^{-/-}mCry2^{-/-}* cells retain the ability to respond to ET-1 treatment or a serum shock with instantaneous induction of *mPer1* and *mPer2* gene expression (16). Thus, as in the SCN and peripheral tissues in intact animals, *mCry* genes are indispensable for generation of molecular rhythm in stimulated cultured mouse fibroblasts.

To investigate whether the periodicity of peripheral clocks is an intrinsic property of the peripheral oscillator or whether it is instigated by cues from the SCN, we have measured temporal expression patterns of the *dbp* gene in immortalized MEFs from *mCry1* and *mCry2* single-mutant mice, known for their short ($\tau = 22.5$ hours) and long ($\tau = 24.6$ hours) free-running periodicity of locomotor activity, respectively (18, 20, 23). The periodicity of *dbp* mRNA oscillation in *mCry1^{-/-}* MEFs, although weak, is about 2 to 4 hours shorter than in *mCry2^{-/-}* MEFs (Fig. 3, D and E). This indicates that mCRY-mediated control over the pace of biological clockwork is not restricted to the central pacemaker in the SCN, but holds for circadian oscillators in any mammalian tissue.

Finally, we measured DBP protein oscillation patterns in serum shock-stimulated MEFs. Robust oscillation of nuclearly localized DBP was observed in wild-type and *mCry2^{-/-}* MEFs (Fig. 4) (26). In *mCry1^{-/-}* cells, nuclear DBP levels remained high after a brief initial nadir. This finding not only

confirms the unexpected pattern of *dbp* gene expression in these cells but also emphasizes the weakness of *mCry2*-mediated oscillations.

As expected on the basis of constant high levels of *dbp* mRNA, nuclei of *mCry1^{-/-}mCry2^{-/-}* cells were positive at any time. For

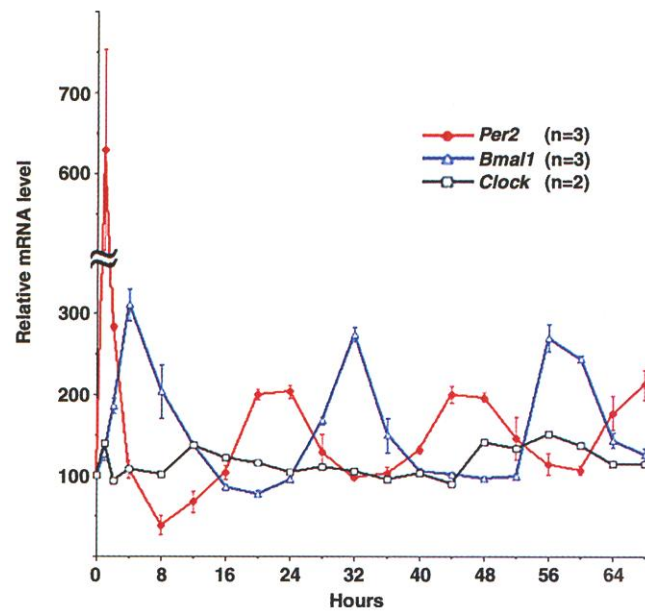


Fig. 1. Temporal expression profiles of clock genes in rat-1 fibroblasts after ET-1 treatment: Quantification of temporal changes in *Per2*, *Bmal1*, and *Clock* mRNAs. Basal levels of each mRNA (at time point 0) were arbitrarily set to 100. Results shown are means \pm SEM; n = number of experiments.

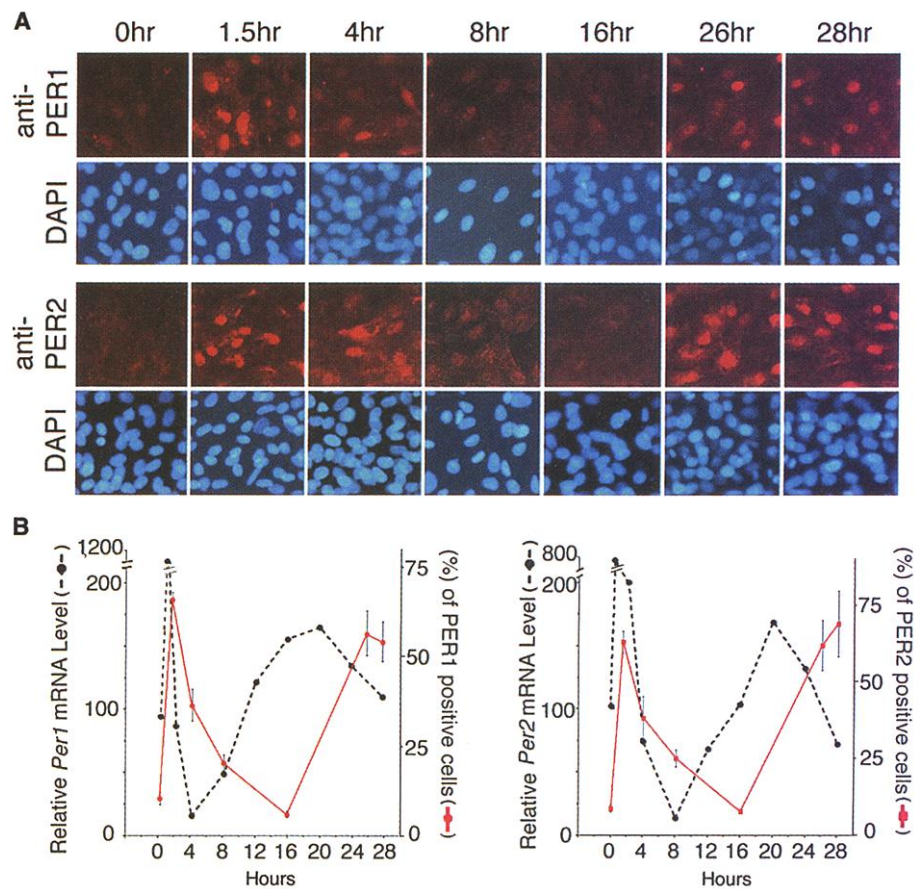


Fig. 2. Temporal PER1 and PER2 protein expression profiles in ET-1-treated rat-1 fibroblasts and comparison with corresponding mRNA expression profiles. (A) Immunofluorescence showing accumulation of PER1 and PER2 proteins in nuclei of ET-1-treated rat-1 fibroblasts. (B) Percentages of cells positive for antibodies to PER1 and PER2 (counted in 100 to 200 DAPI-stained nuclei) at the indicated times. For comparison, relative mRNA levels of *Per1* and *Per2* are shown as broken lines. Results shown are means \pm SEM (three independent experiments).

REPORTS

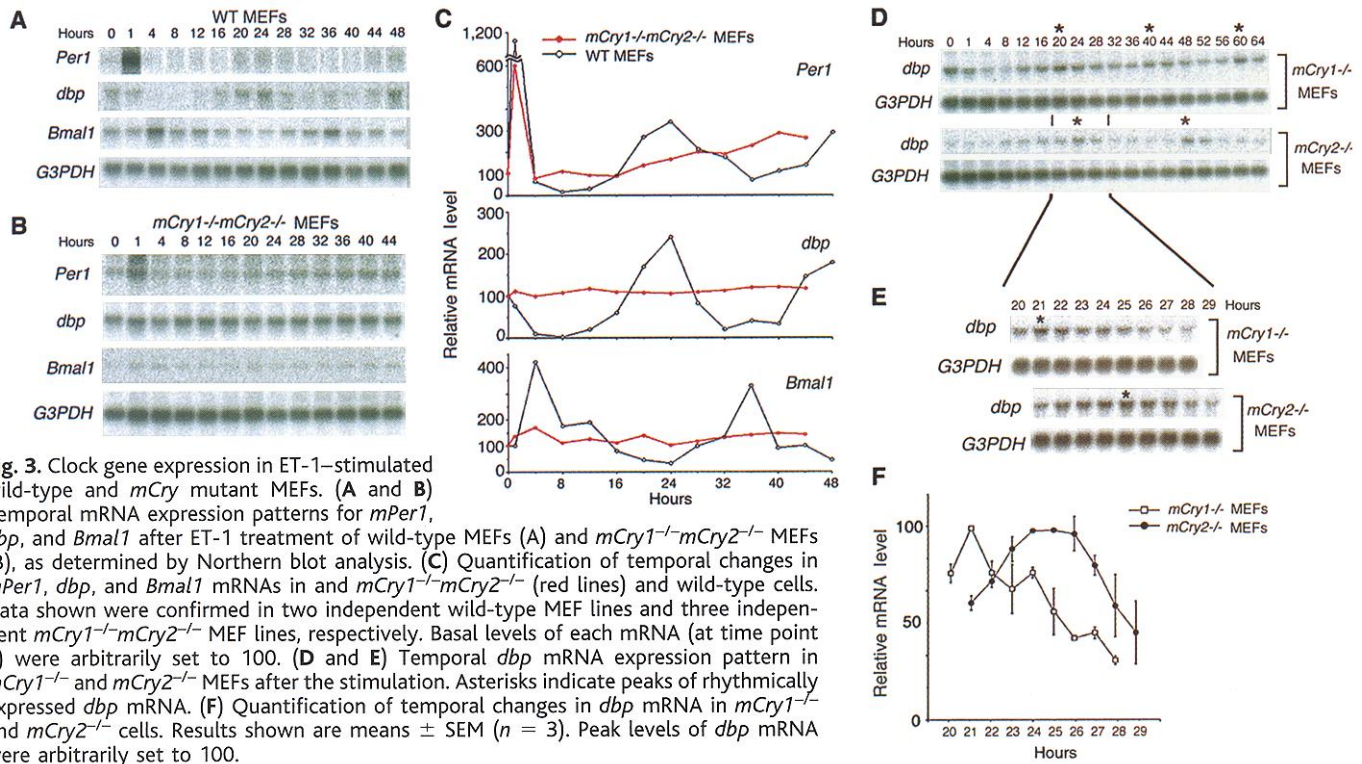


Fig. 3. Clock gene expression in ET-1-stimulated wild-type and *mCry* mutant MEFs. (A and B) Temporal mRNA expression patterns for *mPer1*, *dbp*, and *Bmal1* after ET-1 treatment of wild-type MEFs (A) and *mCry1*^{-/-}*mCry2*^{-/-} MEFs (B), as determined by Northern blot analysis. (C) Quantification of temporal changes in *mPer1*, *dbp*, and *Bmal1* mRNAs in and *mCry1*^{-/-}*mCry2*^{-/-} (red lines) and wild-type cells. Data shown were confirmed in two independent wild-type MEF lines and three independent *mCry1*^{-/-}*mCry2*^{-/-} MEF lines, respectively. Basal levels of each mRNA (at time point 0) were arbitrarily set to 100. (D and E) Temporal *dbp* mRNA expression pattern in *mCry1*^{-/-} and *mCry2*^{-/-} MEFs after the stimulation. Asterisks indicate peaks of rhythmically expressed *dbp* mRNA. (F) Quantification of temporal changes in *dbp* mRNA in *mCry1*^{-/-} and *mCry2*^{-/-} cells. Results shown are means ± SEM (*n* = 3). Peak levels of *dbp* mRNA were arbitrarily set to 100.

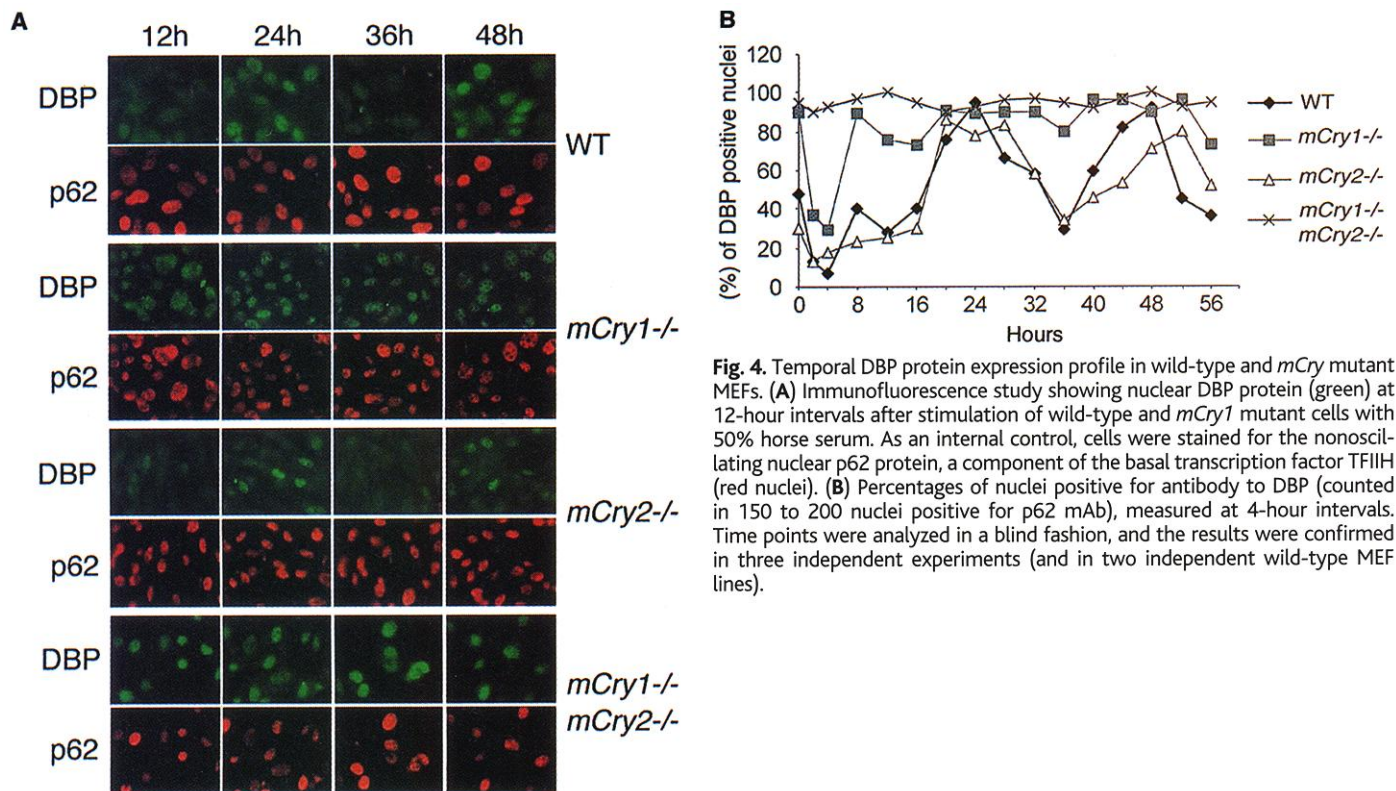


Fig. 4. Temporal DBP protein expression profile in wild-type and *mCry* mutant MEFs. (A) Immunofluorescence study showing nuclear DBP protein (green) at 12-hour intervals after stimulation of wild-type and *mCry1* mutant cells with 50% horse serum. As an internal control, cells were stained for the nonoscillating nuclear p62 protein, a component of the basal transcription factor TFIID (red nuclei). (B) Percentages of nuclei positive for antibody to DBP (counted in 150 to 200 nuclei positive for p62 mAb), measured at 4-hour intervals. Time points were analyzed in a blind fashion, and the results were confirmed in three independent experiments (and in two independent wild-type MEF lines).

all cell lines tested, the appearance of nuclear DBP largely coincided with the (ET-1-mediated) *dbp* mRNA expression profile. These findings suggest that, as in the SCN, DBP is rapidly synthesized and translocated into the nucleus (27).

Taken together, our data indicate that the molecular makeup of the peripheral circadian oscillator in cultured fibroblasts is similar to that of the master oscillator in the SCN. The same set of circadian genes is assembled into positive and negative transcription-transla-

tion feedback loops. The mRNA expression profiles for these circadian genes display an “SCN-like” temporal expression profile as well as phase relationship, and, at least for *mPER1*, *mPER2*, and DBP, the delay between onset of transcription and nuclear ap-

pearance of the corresponding gene product is comparable to that in the SCN. Moreover, the homozygous inactivation of one or both *mCry* genes—known to accelerate, retard, or even abolish the biological clock in the SCN (18, 20, 23)—affects the peripheral oscillator to a similar extent. Thus, the peripheral oscillator in immortalized cultured fibroblasts constitutes a bona fide in vitro model for the molecular oscillator in the SCN, and could potentially allow the use of skin fibroblasts as a means of identifying clock gene defects in patients with circadian disorders.

Although peripheral clocks in the intact mouse possess some degree of autonomy, as is evident from the uncoupling of entrainment of peripheral and master clocks by glucocorticoid administration or restricted feeding (6–8), they differ from the master clock in the SCN in one important aspect. Unlike in cultured SCN slices, rhythmic clock gene expression in cultured peripheral organs/tissues and fibroblasts is dampened after a number of days (9). Because, as we have shown, the molecular makeup of the core oscillator of master and peripheral clocks is identical, the mechanism that allows the master clock to keep on ticking remains to be identified.

References and Notes

1. J. Dunlap, *Cell* **96**, 271 (1999).
2. M. W. Young, *Science* **288**, 451 (2000).
3. N. Cermakian, P. Sassone-Corsi, *Nature Rev. Mol. Cell Biol.* **1**, 59 (2000).
4. L. P. Shearman *et al.*, *Science* **288**, 1013 (2000).
5. R. G. Foster, *Neuron* **20**, 829 (1998).
6. A. Balsalobre *et al.*, *Science* **289**, 2344 (2000).
7. F. Damiola *et al.*, *Genes Dev.* **14**, 2950 (2000).
8. K. A. Stokkan *et al.*, *Science* **291**, 490 (2001).
9. S. Yamazaki *et al.*, *Science* **288**, 682 (2000).
10. A. Balsalobre, F. Damiola, U. Schibler, *Cell* **93**, 929 (1998).
11. K. Yagita and H. Okamura, *FEBS Lett.* **465**, 79 (2000).
12. M. Akashi and E. Nishida, *Genes Dev.* **14**, 645 (2000).
13. Rat-1 fibroblasts were cultured as described (10). Before stimulation, cells were cultured for 3 to 4 days in medium containing 5% fetal bovine serum. Cells were stimulated by brief treatment (2 hours) with medium containing either endothelin-1 (final concentration 30 nM, Sigma), after which medium was replaced by serum-free Dulbecco's modified Eagle's medium (Nacalai Tesque, Kyoto, Japan).
14. M. Yanagisawa *et al.*, *Nature* **332**, 411 (1988).
15. T. Kuwaki *et al.*, *Prog. Neurobiol.* **51**, 545 (1997).
16. See *Science* Online (www.sciencemag.org/cgi/content/full/292/5515/278/DC1).
17. Northern blot analysis was performed as described (11). Probes of *Per1*, *Per2*, and *dbp* were prepared as described (11). For *Clock* and *Bmal1*, full-length cDNAs of *hClock* and *hBmal1* (27) were digested by Xba I and Sma I, respectively. Fragments of *hClock* (base pairs 364 to 1084 of *hClock* cDNA) and *hBmal1* (base pairs 687 to 1506 of *hBmal1* cDNA) were used for the templates. G3PDH (Clontech) was used as a control. Probes were labeled with [³²P]deoxycytidine triphosphate using a TaKaRa random primer labeling kit (TaKaRa, Tokyo, Japan). Hybridization was performed at 42°C for 16 hours, and membranes were washed twice in 0.2× SSC/0.1% SDS at 60°C for 30 min. Membranes were exposed to an imaging plate and analyzed by BAS 5000 (Fuji Film, Tokyo, Japan). For rehybridization purposes, old probes were removed by treatment of membranes with a preheated (80°C) solution containing 1% SDS/0.1× SSC for 3 min.
18. H. Okamura *et al.*, *Science* **286**, 2531 (1999).
19. Y. Ishida *et al.*, *J. Neurosci. Res.*, in press.

20. M. H. Vitaterna *et al.*, *Proc. Natl. Acad. Sci. U.S.A.* **96**, 12114 (1999).
21. M. D. Field *et al.*, *Neuron* **25**, 437 (2000).
22. Immunofluorescence was performed as described (28). Rabbit polyclonal antibodies to mPER1 (28) (affinity purified, 1:200) and mPER2 (affinity purified, 1:200; ADI, San Antonio, TX) were used as primary antibodies. Cy3-conjugated antibody to rabbit IgG (1:2000; Amersham) was used as a secondary antibody. Nuclear staining was performed with 4',6'-diamidino-2-phenylindole (DAPI).
23. G. T. J. van der Horst *et al.*, *Nature* **398**, 627 (1999).
24. Spontaneously immortalized MEFs from *mCry1^{-/-}*, *mCry2^{-/-}*, and *mCry1^{-/-}mCry2^{-/-}* mice were cultured as described (28). Stimulation procedures using ET-1 (final concentration 30 nM) or 50% horse serum (Gibco BRL) were as described (14).
25. K. Yagita, F. Tamanini, G. T. J. van der Horst, H. Okamura, data not shown.
26. Immunofluorescence was performed as described

(28). Rabbit polyclonal antibody to DBP (1:2500) and p62 mouse monoclonal antibody (mAb; 1:3000) were used as primary antibodies. Fluorescein isothiocyanate-conjugated antibody to rabbit IgG (1:2000; Amersham) and Cy3-conjugated antibody to mouse IgG (1:800; Jackson ImmunoResearch) were used as secondary antibodies.

27. S. Yamaguchi *et al.*, *Mol. Cell. Biol.* **20**, 4773 (2000).
28. K. Yagita *et al.*, *Genes Dev.* **14**, 1353 (2000).
29. We thank U. Schibler, J. Ripperger, and J. M. Egly for antibodies, and M. Yasuda for technical support. Supported in part by grants from the Special Coordination Funds of the Science and Technology Agency of Japan, a Grant-in-Aid for Scientific Research on Priority Areas of the Ministry of Education, Science, Sports and Culture of Japan, Ministry of Welfare of Japan, Mitsubishi Foundation, and a Spinoza premium from the Netherlands Organization for Scientific Research.

2 February 2001; accepted 15 March 2001

Forecasting Agriculturally Driven Global Environmental Change

David Tilman,^{1*} Joseph Fargione,¹ Brian Wolff,¹ Carla D'Antonio,² Andrew Dobson,³ Robert Howarth,⁴ David Schindler,⁵ William H. Schlesinger,⁶ Daniel Simberloff,⁷ Deborah Swackhamer⁸

During the next 50 years, which is likely to be the final period of rapid agricultural expansion, demand for food by a wealthier and 50% larger global population will be a major driver of global environmental change. Should past dependences of the global environmental impacts of agriculture on human population and consumption continue, 10⁹ hectares of natural ecosystems would be converted to agriculture by 2050. This would be accompanied by 2.4- to 2.7-fold increases in nitrogen- and phosphorus-driven eutrophication of terrestrial, freshwater, and near-shore marine ecosystems, and comparable increases in pesticide use. This eutrophication and habitat destruction would cause unprecedented ecosystem simplification, loss of ecosystem services, and species extinctions. Significant scientific advances and regulatory, technological, and policy changes are needed to control the environmental impacts of agricultural expansion.

During the first 35 years of the Green Revolution, global grain production doubled, greatly reducing food shortages, but at high environmental cost (1–5). In addition to its effects on greenhouse gases (1, 6, 7), agriculture affects

ecosystems by the use and release of limiting resources that influence ecosystem functioning (nitrogen, phosphorus, and water), release of pesticides, and conversion of natural ecosystems to agriculture. These sources of global change may rival climate change in environmental and societal impacts (2, 8). Population size and per capita consumption are assumed to be the two greatest drivers of global environmental change. Humans currently appropriate more than a third of the production of terrestrial ecosystems and about half of usable freshwaters, have doubled terrestrial nitrogen supply and phosphorus liberation, have manufactured and released globally significant quantities of pesticides, and have initiated a major extinction event (2–4, 8–10). Global population, which increased 3.7-fold during the 20th century, to 6 billion people (11), is forecast to increase to 7.5 billion by the year 2020 and to about 9 billion by 2050 (12). Constant-dollar global per capita

¹Department of Ecology, Evolution and Behavior, University of Minnesota, 1987 Upper Buford Circle, St. Paul, MN 55108, USA. ²Department of Integrative Biology, University of California, Berkeley, CA 94720, USA. ³Department of Ecology & Evolutionary Biology, Princeton University, Princeton, NJ 08540, USA. ⁴The Oceans Program, Environmental Defense, and the Ecosystems Center, Marine Biological Lab, Woods Hole, MA 02543, USA. ⁵University of Alberta, Z-811 Biological Sciences Building, Edmonton, Alberta, T6G 2E9, Canada. ⁶The Phytotron, Duke University, Durham, NC 27708, USA. ⁷Department of Ecology & Evolutionary Biology, University of Tennessee, Knoxville, TN 37996, USA. ⁸Environmental and Occupational Health, University of Minnesota, 420 Delaware Street SE, Minneapolis, MN 55455, USA.

*To whom correspondence should be addressed. E-mail: tilman@ter.umn.edu